LA-4385-TR

LOS ALAMOS SCIENTIFIC LABORATORY
of the
University of California
LOS ALAMOS • NEW MEXICO

Photofission of Thorium-232, Uranium-238, Plutonium-238, Plutonium-240, and Plutonium-242 and Structure of the Fission Barrier

UNITED STATES
ATOMIC ENERGY COMMISSION
CONTRACT W-7405-ENG. 36

This translation has been prepared in response to a specific request; it is being given standard distribution because of its relevance to the nuclear energy program. Reasonable effort has been made to ensure accuracy but no guarantee is offered.

Printed in the United States of America. Available from
Clearinghouse for Federal Scientific and Technical Information
National Bureau of Standards, U. S. Department of Commerce
Springfield, Virginia 22151
Price: Printed Copy $3.00; Microfiche $0.65

Distributed: July 1970

LA-4385-TR
UC-34, PHYSICS
TID-4500

LOS ALAMOS SCIENTIFIC LABORATORY
of the
University of California
LOS ALAMOS • NEW MEXICO

Photofission of Thorium-232, Uranium-238, Plutonium-238, Plutonium-240, and Plutonium-242 and Structure of the Fission Barrier

by

N. S. Rabotnov, G. N. Smirenkin,
A. S. Soldatov, and L. N. Usachev,
Institute of Physics and Energetics, Academy of Sciences, USSR;
S. P. Kapitsa and Iu. M. Tsipeniuk,
Institute of Physical Problems, Academy of Sciences, USSR

Source: Institute of Physics and Energetics report FEI-170, 1969.

Translated by

Helen J. Dahlby

PHOTOFISSION OF THORIUM-232, URANIUM-238, PLUTONIUM-238, PLUTONIUM-240, AND PLUTONIUM-242 AND STRUCTURE OF THE FISSION BARRIER

by

N. S. Rabotnov, G. N. Smirenkin, A. S. Soldatov,
L. N. Usachev, S. P. Kapitsa and Iu. M. Tsipeniuk

ABSTRACT

Measurements of the angular distributions and fragment yields for photofission of the even-even nuclei ^{232}Th, ^{238}U, ^{238}Pu, ^{240}Pu, and ^{242}Pu near the threshold are reported. Measurements were made in a beam of bremsstrahlung gamma quanta in the 12-MeV microtron of the Institute of Physical Problems of the Academy of Sciences of the USSR in the region of maximum energies, E_{max}, from 5 to 10 MeV. Calculation of the bremsstrahlung spectrum from a 1-mm tungsten target used to reduce the dependence of the total photofission cross section and its angular components on the energy, E, of the gamma quanta is described. The results, which do not fit traditional concepts, indicate the existence of a double-humped fission barrier.

INTRODUCTION

The (γ,f) reaction for gamma-quanta energy near the fission threshold is very attractive in fission physics study for two reasons. First, 5- to 7-MeV photons, apparently, undergo absorption only with E1 and E2 multipolarities on heavy nuclei. For the even-even targets discussed here, this leads to formation of composite nuclei with only two combinations of spin and parity, 1^- and 2^+, and quadrupole absorption must be an order or two less probable. Second, the momenta of the composite nuclei after the absorption of gamma quanta are aligned along the photon beam. In dipole absorption, the alignment is total.

One can describe characteristics of the fission process, by investigating the one-dimensional problem of passage of a particle through a potential barrier of given height. This height is called the fission threshold, although in a precise sense fission is not a threshold reaction.

The first problem in analysis of experimental fission data usually is determination of the height and shape of the fission barrier. For a fissioning nucleus of fixed nucleon composition, the barrier usually depends on the quantum numbers of the state from which the fission occurs, and this fact affects the energy dependence of the differential and total fission cross sections in a predetermined manner. In addition to the spin and parity of the composite nucleus, the barrier can depend substantially on the value of K, the projection of the momentum in the direction of the axis of symmetry of the nucleus, along which the fragments disintegrate. If fission with a definite K value is energetically favorable, the momenta of the fissioning composite nuclei are oriented; this also leads to the appearance of anisotropy in the angular distributions. This anisotropy was first disclosed by Winhold et al.[1] A physical interpretation of this phenomenon sug-

gested by A. Bohr[2] described the concrete mechanism of separation of "chosen" values of K in the fission process. In the passage through the saddle point, much of the energy is concentrated in the deformation potential, the remaining degrees of freedom can be excited by a limited number of processes, and the nucleus fissions through transition states, "fission channels," with determined K values.

This report summarizes the experimental study of the angular distributions of fission fragments of even-even nuclei by bremsstrahlung gamma quanta. Results are given for measurements of the angular distributions of fragments, $W(\theta)$, in the region of limiting energies of the bremsstrahlung spectrum, E_{max} = 5 to 10 MeV, for five nuclei: ^{232}Th, ^{238}U, ^{238}Pu, ^{240}Pu, and ^{242}Pu. Some data for ^{232}Th, ^{238}U, and ^{240}Pu were reported earlier.[3,4] Brief information on our results is contained in a preliminary publication.[5,6]

An intensive reevaluation of the basic concepts of the course of the fission process is underway because of the appearance of the hypothesis of the existence of a second minimum in the potential curve.[7] Its possibilities are discussed in the interpretation of our experimental data, together with the traditional hypotheses of the dependence of fission probability on the quantum characteristics of the fissioning nucleus.

EXPERIMENTAL

The experiment was carried out on the internal target of a 12-MeV high-current microtron of the Institute of Physical Problems of the USSR Academy of Sciences. As in Refs. 3 and 4, the bremsstrahlung target was a 1-mm-thick tungsten plate. The average working current was 50 μA. To filter the electrons from the gamma-quanta beam, a 10-mm-thick aluminum absorber was placed directly behind the target. Glass detectors were used for angular distribution measurements.[8] The detectors and fissioning layer backings were installed in a cassette, which was placed inside the accelerating chamber of the microtron so as not to interfere with the electrons in the preceding orbit. The plane of the layer backings was at an angle of 45° to the axis of the bremsstrahlung gamma-quanta beam (Fig. 1). A detecting device permitted studying two different fissioning substances simul-

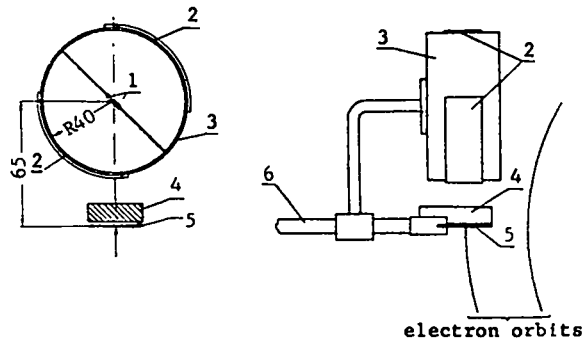

Fig. 1. Experimental device and test geometry. 1. layer of fissioning substance; 2. fission fragment detectors; 3. cassette; 4. aluminum filter; 5. tungsten target; 6. screw-driven probe.

taneously or using double layers of one isotope. The bremsstrahlung target and cassette were rigidly fastened to a screw-driven probe, which permitted remote transfer of the whole experimental device relative to the electron beam. Accuracy of installation of the detector relative to the electron beam was determined by television and was ~ 1 mm.

At various stages, detectors of different configuration and fissioning samples of different thickness were used. Experiments were carried out with sets of rectangular and cylindrical glasses that covered angles from -7.5 to 97.5°. Table I shows the characteristics of the isotopes studied. In the study of ^{232}Th and ^{238}U photofission, foils considerably thicker than the fragment range were used. Other conditions being equal, their use permitted increasing the reading statistics 5 to 7 times relative to a layer 1 mg/cm^2 thick.[8] The angles studied were divided into seven intervals. Scanning each angular interval of the detector under a microscope gave the number of fragments striking in it, N_j, with an accuracy of 0.5 to 2%, as a function of the density of fragment traces.[4]

The inaccuracy in determining the electron beam energy (uncertainty of ΔE_{max}) in our earlier papers[3,4] was taken as ±50 keV; later, when the electron energy was adjusted and controlled by measuring the microtron field by nuclear magnetic resonance, we decreased ΔE_{max} to ±25 keV.

TABLE I

PARAMETERS OF LAYERS OF THE FISSIONING ELEMENTS USED

Isotope studied	Total amount of substance	Thickness of layers	Impurities
^{232}Th - double	2.12 mg	1.35 mg/cm^2	~ 0%
^{238}U - double	1.72 mg	1.1 mg/cm^2	Natural
^{238}U		200 mg/cm^2	In union with ^{235}U 1:200
^{238}Pu - double	0.057 mg	0.036 mg/cm^2	< 0.3%
^{240}Pu	0.144 mg	0.182 mg/cm^2	7.3% ^{239}Pu
^{242}Pu - double	0.700 mg	0.445 mg/cm^2	1.5% ^{240}Pu 2.0% ^{241}Pu

During irradiation the average current of electrons completely absorbed in the target and aluminum filter was continuously recorded. This, incidentally, permitted a determination, from the basic measurements, of $W(\theta)$, the yield of the (γ,f) reaction per unit of electron current, and unit of mass of the studied isotope, $Y(E_{max})$. The error of these measurements was estimated as 15%.

The parameters of the accelerator, a diagram, and specific characteristics of the experiment are described in more detail by Bocharova et al.[4]

MEASUREMENT RESULTS

Angular Distributions of Fragments

Owing to the finite angular resolution, the distribution of the number of counts, N_j, determined directly in experiment cannot be simply identified with the unknown function $W(\theta)$:

$$N_j \sim \iint_{\Omega\Omega_j} W(\theta)\eta(\Psi)d\Omega d\Omega_j \quad , \qquad (1)$$

where $d\Omega$ and $d\Omega_j$ are the elements of the solid angle constructed, respectively, on the vectors coming from the photon's point of escape to the point of the layer in which fission occurred, and from this point to the detector point at which the fragment was recorded; and $\eta(\Psi)$ is the fragment recording efficiency, which depends on the angle of escape from the layer, $\Psi \approx |90^\circ - \theta|$.

In work with layers of the studied isotopes, the thicknesses of which are shown in Table I, the fragment recording efficiency in the region of change acceptable for the geometry used, $0^\circ \leqslant \Psi \leqslant 45^\circ$ ($0^\circ \leqslant \theta \leqslant 90^\circ$) did not depend on the angle, within 1 to 2%. The angular dependence of the fragment recording efficiency in tests with thorium and uranium foils, thick in comparison with the range, is described well by the cosine law, $\eta(\Psi) = \cos\Psi$, which comes from simple geometric considerations.[8]

The mathematical treatment of the results of measurements of N_j is discussed in detail in Refs. 4 and 8. The goal of that analysis is to determine by the method of least squares the coefficients a, b, and c in the angular distribution

$$W(\theta) = a + b\sin^2\theta + c\sin^2 2\theta \quad , \qquad (2)$$

in the very general form describing the spatial distribution of the fragment disintegration probability during dipole and quadrupole photofission. Note that in these calculations, done with an electronic computer, the finite dimensions of the layer of fissioning substance and the angular intervals of the detector are accurately accounted for by the Monte Carlo method. In this, however, the finite dimensions of the electron beam (2 by 4 mm^2) and the angular dependence of the gamma-irradiation intensity were disregarded within the limits of the solid angle isolated by the layer (from the center to the edge of the layer the intensity drops by 10 to 15%). Rough calculation of the electron beam dimensions showed that the values given below for the coefficients a are somewhat too high. The maximum possible error depends on the

value of the coefficients as follows.

a	0.015	0.1	0.6	0.8
Error in %	30	9	0.7	0.2

The coefficient c, on the other hand, is lowered by 2 to 3% on the average, practically independent of its value. The errors caused by the nonuniform "exposure" of the fissioning sample surface are small (~ 1 to 2%) for all values of coefficients of $W(\theta)$. The errors of N_j measurement in the mathematical treatment were summed from the statistical error of the counts and the average scanning error.

The coefficients of the angular distribution of fragments in the normalization a + b = 1 are given in Table II. Figure 2 shows the ratios of the coefficients, b/a and c/b. The ratio $b/a = W(0^\circ)/W(90^\circ) - 1$ characterizes the angular anisotropy of photofission; c/b, the relative contribution of the quadrupole component. Here we give only data obtained with "thin" samples. Information obtained with metallic foils, owing to the distortions in $W(\theta)$ that occur because of the scattering of fragments in thick samples, was used only to determine the relative energy dependence of the total fission yield (see below).

TOTAL YIELD OF THE (γ,f) REACTION

In earlier work on photofission,[9] most of which was carried out in betatrons and synchrotrons, the reaction yield usually was relative to 1R of bremsstrahlung gamma-radiation intensity and a unit of the amount of fissioning substance. Presumably, in measurements on the internal target of a microtron, the problems in measuring the electron current, which are inherent to induction accelerators, do not arise. This affords the possibility of introducing data on the (γ,f) reaction yield, $Y(E_{max})$, in a simpler normalization: as the total number of fissions per second per microampere of electron current per milligram of fissioning substance,

$$Y = F \int W(\theta)\sin\theta d\theta = 2F\left(a + \frac{2}{3}b + \frac{8}{15}c\right) = 2F\nu \quad . \quad (3)$$

The multipliers F and ν depend on E_{max}. Experimental data on the total yield, $Y(E_{max})$, obtained from measurements of layers of fissioning samples, are given in the last column of Table II. The whole set of data on $Y(E_{max})$, including the results obtained with metallic thorium and uranium foils, is shown in Fig. 3.

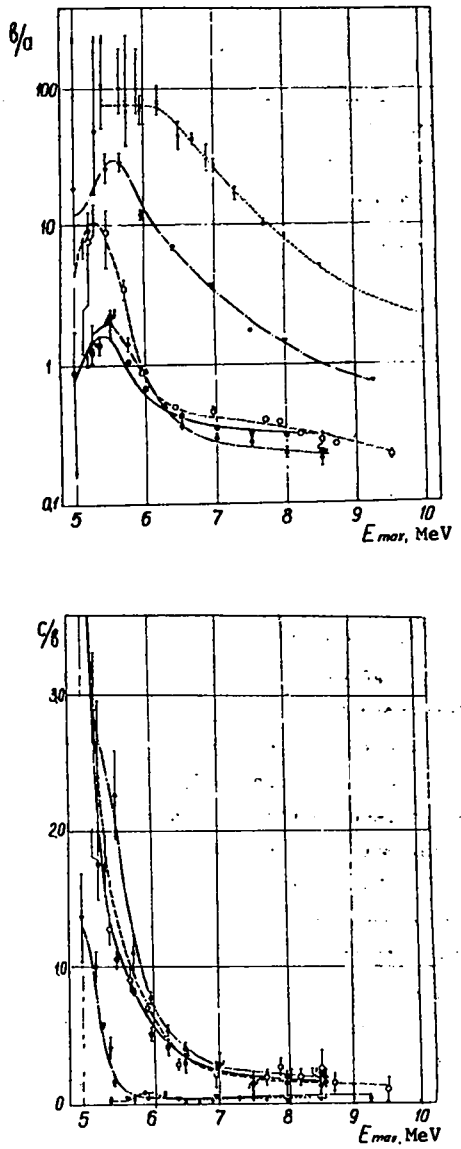

Fig. 2. Ratios of coefficients b/a and c/b as a function of E_{max}. x for ^{232}Th; ∇ for ^{238}U; Δ, for ^{238}Pu; o, for ^{240}Pu; •, for ^{242}Pu.

ANGULAR COMPONENTS OF YIELD

Knowledge of the coefficients a, b, and c permits determining the contribution of the individual yield components, Y_a, Y_b, and Y_c, for which the angular dependence corresponds to the three components, isotropic, dipole, and quadrupole, in

TABLE II

PARAMETERS OF ANGULAR DISTRIBUTIONS OF FRAGMENTS

E_{max} MeV	a	b	c	Y fissions / mg μA sec
I	2	3	4	5
		Th^{232}		
5.2	-	-	-	$4.5.10^{-5}$
5.4	0,009 ± 0.009	0.99I ± 0.027	0.030 ± 0,025	0.0024
5,65	0.0II ± 0.005	0.989 ± 0.007	-0.005 ± 0.006	0.059
5.75	0.0I5 ± 0.0I0	0.985 ± 0.034	0,033 ± 0.033	0.062
5.9	0.0I0 ± 0.005	0,990 ± 0.0I6	0.084 ± 0.0I4	0,20
5.95	0.0I4 ± 0.004	0.986 ± 0,009	0.074 ± 0,0I0	0.32
6.2	0.0I2 ± 0,003	0.988 ± 0,0I0	0,079 ± 0.0I0	0,79
6.5	0.022 ± 0.005	0,978 ± 0,0I5	0.022 ± 0,0I4	5.4
6.7	0.023 ± 0.002	0.977 ± 0.009	0,009 ± 0,008	9.8
6,9	0.032 ± 0.007	0,968 ± 0,024	0.020 ± 0.022	7.7
7,0	0.036 ± 0.004	0.964 ± 0.0I3	0,038 ± 0.0I2	I3.5
7.3	0.056 ± 0.006	0.944 ± 0.020	0.03I ± 0,0I7	I9.5
7.7	0.088 ± 0.005	0.9I2 ± 0.0I5	0.028 ± 0,0I3	40.5
8.0	0.I09 ± 0.006	0.89I ± 0.0I3	0.026 ± 0,0I2	35
8.5	0.I64 ± 0.004	0.836 ± 0.008	0,0I7 ± 0.008	7I
I0.0	0.304 ± 0.009	0.696 ± 0,0I4	-0,03I ± 0,0I4	-
		U 238		
5.0	0.052 ± 0.I00	0.948 ± 0.I64	I.296 ± 0.205	0.0007I
5,2	0.I00 ± 0.035	0.900 ± 0.06I	0.9I0 ± 0.080	0.0042
5,3	0.020 ± 0.035	0.980 ± 0.064	0.566 ± 0.076	0.0I20
5,4	0,007 ± 0,024	0.993 ± 0.059	0.4I2 ± 0.066	0.030
5,45	0.038 ± 0,009	0.962 ± 0.0I7	0.I55 ± 0.02I	0.044
5,65	0.034 ± 0.005	0.966 ± 0.0II	0.040 ± 0.0I0	0,27
5,95	0.078 ± 0.005	0.922 ± 0.0I4	0.039 ± 0.0I4	I,7
6,4	0,I27 ± 0.004	0.873 ± 0.009	0.034 ± 0.008	6.0
6,95	0.2I3 ± 0.004	0.787 ± 0.008	0,047 ± 0.008	24.0
7,5	0.364 ± 0.006	0.636 ± 0.0I0	0.024 ± 0.0II	47.0
8,0	0.40I ± 0.005	0.599 ± 0.006	0.0I4 ± 0.007	74.0
9.25	0,570 ± 0.006	0.430 ± 0.007	0.0I3 ± 0.007	-
		Pu^{238}		
5.25	0.408 ± 0.I03	0,592 ± 0,I30	I.4I2 ± 0.I39	0.04I
5,5	0.330 ± 0.063	0,670 ± 0.084	I.5I3 ± 0,II2	0,I4
5,75	0,4I4 ± 0.037	0.586 ± 0,046	0,654 ± 0,055	0.47
6,0	0,526 ± 0,0II	0.474 ± 0.0I6	0.370 ± 0,0I8	I.7
6,25	0.666 ± 0.008	0.334 ± 0,0II	0.I80 ± 0.0I3	5.9
6.5	0,733 ± 0,0I2	0,267 ± 0.0I6	0,080 ± 0.0I8	II
7.0	0.772 ± 0.0II	0.228 ± 0,0I6	0,068 ± 0.0I7	56
7.5	0.785 ± 0,0I2	0.2I5 ± 0.0I7	0,032 ± 0,0I9	80
8,0	0.8I3 ± 0,0I3	0.I87 ± 0.0I7	0,029 ± 0.0I8	I60
8,5	0.828 ± 0,0I5	0.I72 ± 0.020	0,023 ± 0.022	270

TABLE II. CONTINUED

I	2	3	4	5
		Pu^{240}		
5.0*)	0 ± 0.200	0 ± 0.200	I ± 0.200	0.008I
5.2	0.II5 ± 0.097	0.885 ± 0.III	2.58 ± 0.I5	0.047
5.45	0.I02 ± 0.044	0.898 ± 0.056	I.I47 ± 0.070	0.I5
5.65	0.222 ± 0.034	0.778 ± 0.042	0.7I0 ± 0.052	0.49
5.95	0.533 ± 0.0I0	0.467 ± 0.0II	0.33I ± 0.0I3	2.3
6.4	0.670 ± 0.0I2	0.330 ± 0.0I2	0.996 ± 0.0I3	II.5
6.95	0.689 ± 0.025	0.3II ± 0.027	0.067 ± 0.029	40
7.7	0.7I6 ± 0.0I2	0.284 ± 0.0I6	0.055 ± 0.0I7	II5
7.9	0.725 ± 0.0I2	0.275 ± 0.0I6	0.074 ± 0.0I8	I45
8.2	0.762 ± 0.0I0	0.238 ± 0.0I4	0.046 ± 0.0I5	I80
8.5	0.779 ± 0.020	0.22I ± 0.027	0.057 ± 0.029	240
8.7	0.79I ± 0.009	0.209 ± 0.0I2	0.032 ± 0.0I4	230
9.5	0.822 ± 0.0II	0.I78 ± 0.0I4	0.0I9 ± 0.0I6	680
		Pu^{242}		
5.0	0.532 ± 0.308	0.468 ± 0.372	3.702 ± 0.424	0.0055
5.25	0.448 ± 0.053	0.552 ± 0.068	0.965 ± 0.082	0.056
5.35	0.4I8 ± 0.046	0.582 ± 0.059	I.0I8 ± 0.069	-
5.5	0.3I0 ± 0.022	0.690 ± 0.029	0.734 ± 0.034	0.26
5.75	0.488 ± 0.008	0.5I2 ± 0.0I0	0.422 ± 0.0I2	I.0
6.0	0.598 ± 0.0II	0.402 ± 0.0I6	0.207 ± 0.0I8	2.7
6.25	0.669 ± 0.0I2	0.33I ± 0.0I7	0.I38 ± 0.0I9	8.8
6.5	0.700 ± 0.009	0.300 ± 0.0I3	0.I22 ± 0.0I4	I7
7.0	0.740 ± 0.005	0.260 ± 0.007	0.075 ± 0.008	50
7.5	0.754 ± 0.005	0.246 ± 0.007	0.036 ± 0.008	I05
8.0	0.766 ± 0.006	0.234 ± 0.008	0.047 ± 0.009	I75
8.5	0.8I4 ± 0.005	0.I86 ± 0.007	0.042 ± 0.008	225

*) In this case $W(\theta)$ is described by the pure quadrupole distribution $\sim \sin^2 2\theta$; therefore, coefficient c in the normalization used has no meaning and is taken as equal to unity.

Eq. (2). Their sense is understood from the determinations

$$Y = Y_a + Y_b + Y_c, \quad \frac{dY}{d\Omega} = \frac{1}{4\pi\nu} \cdot Y \cdot W(\theta), \qquad (4)$$

$$Y_a = \frac{a}{\nu} \cdot Y, \; Y_b = \frac{2}{3}\frac{b}{\nu} \cdot Y, \; Y_c = \frac{8}{15}\frac{c}{\nu} \cdot Y \quad .$$

The dependence of Y_i on E_{max} are given in Fig. 3, together with data on the total yield. The experimental points of $Y_i(E_{max})$ were found by Eqs. (4) from the values of the coefficients of $W(\theta)$, which are given in Table II, and the smoothed curve of the total yield (see below). The ~15% measurement error in $Y(E_{max})$ is not included in the error in Y_i shown in Fig. 3.

THE REDUCTION OF CROSS SECTIONS AS FUNCTIONS OF PHOTON ENERGY

Our experiments permit direct determination of only the integral characteristics, yield and angular components of yield as a function of the maximum energy of the bremsstrahlung radiation spectrum. For a theoretical analysis, it is of far greater value to offer data on the fission cross section, $\sigma_f(E)$, and its angular components; these can be calculated by solution of the Volterra integral equation of the first type,

$$Y(E_{max}) = c \int_0^{E_{max}} \sigma(E) \cdot f(E, E_{max}) dE, \qquad (5)$$

with experimentally determined left-hand parts. The main body of Eq. (5), $f(E, E_{max})$, is the number of gamma quanta in the energy interval E, E + dE for one electron; the coefficient c ahead of the integral does not depend on E_{max}.

To solve Eq. (5), one must first know with sufficient reliability the gamma-quanta spectrum

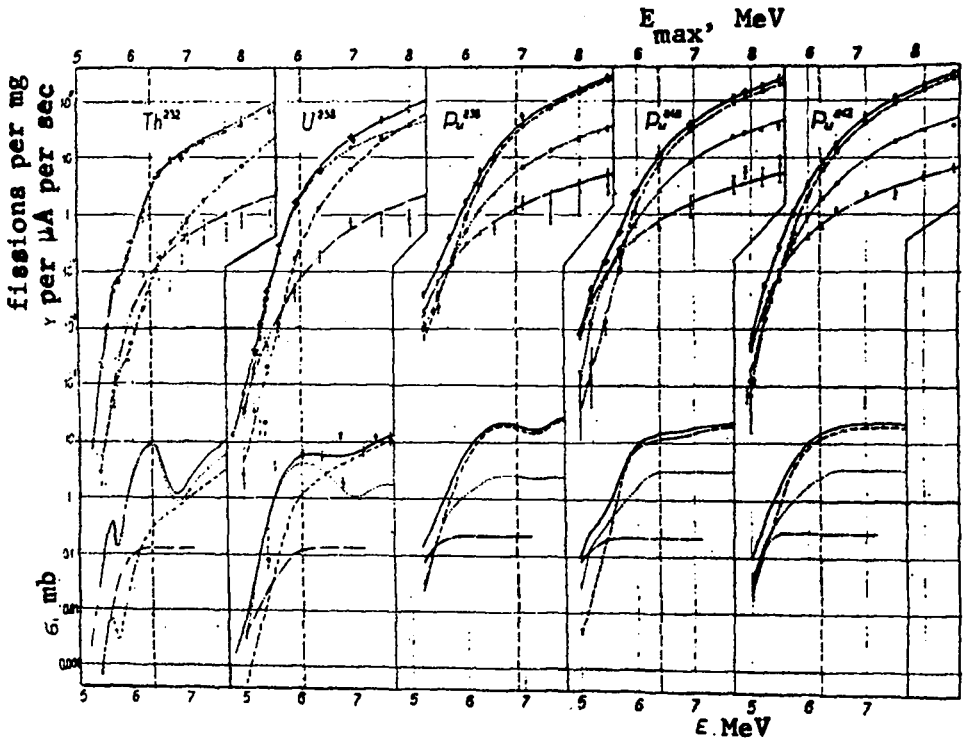

Fig. 3. Energy dependence of total yield $Y(E_{max})$ (o) and its angular components $Y_a(E_{max})$ (•), $Y_b(E_{max})$ (▲), and $Y_c(E_{max})$ (x). Below - dependences, obtained using Eq. (5), of total cross section, $\sigma_{\gamma f}(E)$, (————), and its angular components $\sigma_a(E)$ (- - -), $\sigma_b(E)$ (----), and $\sigma_c(E)$ (-.-.-.) on energy of gamma quanta. Points for $\sigma_{\gamma f}$ in ^{238}U are from Ref. 16. Vertical dotted lines denote neutron binding energy in the corresponding nucleus.

of the bremsstrahlung radiation $f(E,E_{max})$ from the thick target.

GAMMA-QUANTUM SPECTRUM

The spectra of bremsstrahlung radiation from thick targets has not been studied in enough detail to permit using an interpolation of experimental data to establish the function $f(E,E_{max})$. The single possible path is calculation. In our earlier papers,[3,4] to analyze measurement results we used the approximate relation

$$f(E,E_{max}) \sim (E_{max} - E)^2 \quad , \qquad (6)$$

obtained on the rough assumption of a uniform intensity distribution of the gamma radiation forward, J, over the thickness of the target, t. This assumption does not account for an important effect, the multiple scattering of electrons, which leads to a significant decrease in $dJ(0^\circ,t)/dt$ with increase in t. Lowson[10] showed that $J(0^\circ,t) \sim$ ln 950 t, where the thickness t is expressed in units of the radiation length. This equation, which agrees well with experiment,[11] was also incorporated into the more corrective calculations of the gamma-quanta bremsstrahlung spectrum.

The spectrum sought was found by summation of the spectra of the separate target layers, taken in the form of integral Schiff distributions weighted to account for the logarithmic dependence of the intensity. The calculation was carried out using two assumptions: with electron energy ionization losses only, and with average radiation losses. In Fig. 4, the calculations are compared with experiment in the gamma-quanta energy region, E, from 2 MeV to E_{max} for two values of the spectrum's limiting energy, E_{max} = 4.55 and 9.65 MeV, and three tungsten target thicknesses, t = 0.12, 0.25, and 3.0 mm. From the data given it follows that:

1. Taking into account the radiation losses, in

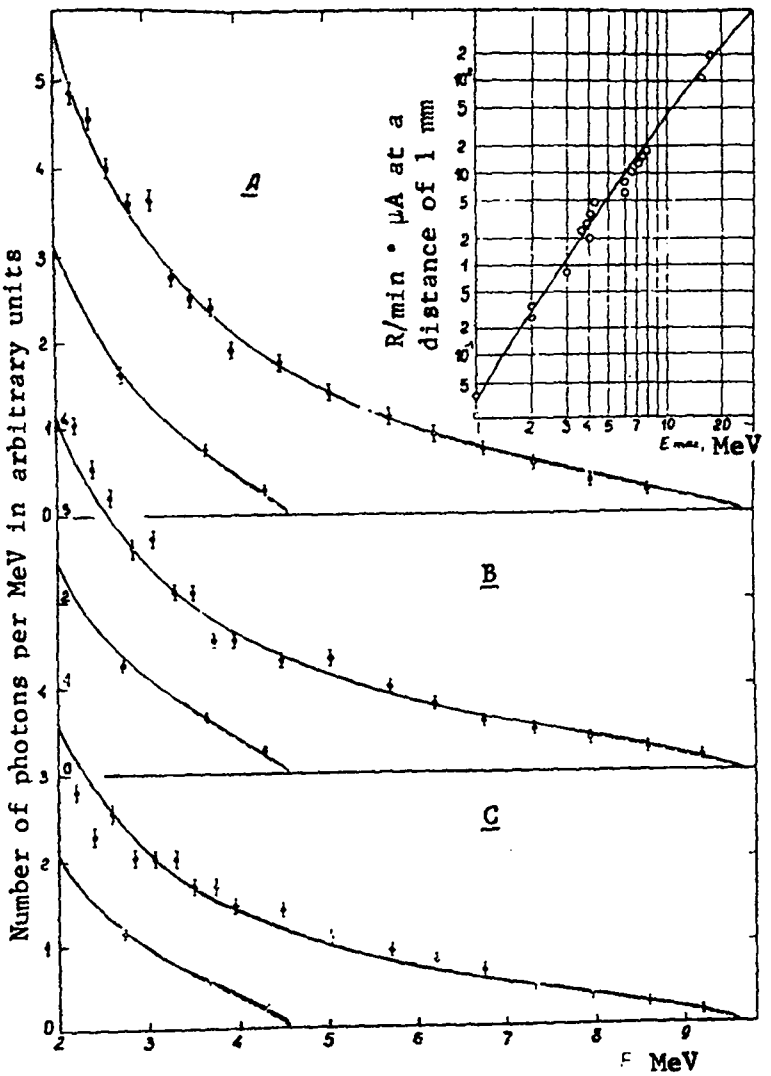

Fig. 4. Calculated spectra of bremsstrahlung radiation γ-quanta forward, from tungsten targets (A) 3-mm, (B) 0.25-mm, and (C) 0.12-mm thick compared with experimental spectra.[11] Solid line, calculation without taking average losses in irradiation into account; dotted line, taking average losses in irradiation into account. Insert shows energy dependence of intensity of γ-radiation forward.[12]

accord with Lowson,[10] does not substantially change the gamma-quantum spectrum;

2. The results of calculation agree well with experiment over a wide range of E_{max} and t; this range is completely satisfactory for our work;

3. In the gamma-quanta energy region important for the fission process, ($\geq$ 5 MeV), the spectrum is nearly linear, in contrast to the parabolic dependence, Eq. (6), assumed earlier.

The distribution, $f_1(E,E_{max})$, thus calculated was normalized to the experimentally studied path of the intensity of the total gamma-radiation forward, $J(0^\circ, E_{max})$:

$$J(0^\circ,E_{max}) = A(E_{max}) \int_0^{E_{max}} E \cdot \gamma(E) \cdot f_1(E,E_{max}) dE \quad , \quad (7)$$

where $J(0^\circ,E_{max})$ is the dependence for an analogous "thick" target depicted in the insert to Fig. 4,[12]

and $\gamma(E)$ takes into account the self-absorption of gamma-quanta in the target and the relation between the gamma-radiation flux and the dose rate, expressed in roentgens per unit of time. We consider that as a result of this normalization the functional dependence of the photon yield's energy distribution, $f(E,E_{max}) = A(E_{max}) \cdot f_1(E,E_{max})$, is obtained. However, the accuracy of the absolute yield value is hardly better than 30%. Therefore we were limited to finding the relative path of $\sigma(E)$. Note that the absorption of gamma quanta in the aluminum filter, as well as the bremsstrahlung radiation from it, arising from incomplete loss of electron energy in the target, appears only in the unimportant deep subbarrier region of gamma-quantum energies.

CALCULATION OF CROSS SECTIONS

The photofission cross section, $\sigma(E)$, and its angular components, $\sigma_a(E)$, $\sigma_b(E)$, and $\sigma_c(E)$, are the unknown functions of integral Eq. (5), the main part of which is the gamma-quanta spectrum, $f(E,E_{max})$, determined above. To find the cross sections as functions of the photon energy, we used the method of matrix treatment proposed by Nozik and Turchin.[13] This method permits solving Eq. (5) with experimentally determined left-hand parts, using the method of maximum probabilities. Having at our disposition a program of calculations, we calculated values of $Y(E_{max})$ equidistant in energy, using the electronic computer. Our experiment does not satisfy this condition. So that we could use the indicated program, we interpolated the experimental data by drawing smooth curves through the experimental points, dividing the interesting region, E_{max} = 5.0 to 8.5 MeV, into equal 0.1-MeV intervals.

Before turning to the results of the calculations, let us consider the accuracy of such a treatment applicable to the properties of the studied dependence.

1. Finding the unknown functions of the integral Eq. (5) belongs to the class of incorrectly posed problems. Uncertainties caused by the "oscillation" of the solutions are inherent to problems of this type. This property of our treatment of the experimental data demanded caution in interpretation of the observed irregular behavior of the derived functions, $\sigma(E)$.

2. The matrix method of solution of Eq. (5) is a more complete modification, mathematically, than differentiation of the curve $Y(E_{max})$, the so-called method of difference of photons. The relative error of the differentiation, roughly speaking, is inversely proportional to $(d \ln Y/dE_{max})$, from which we can conclude that, despite the overall increase in the statistics of counts with increase in E_{max}, the accuracy of determination of the cross section near the plateau will be worse than in the larger part of the subbarrier section.

3. The accuracy of calculation of the individual cross-section components depends considerably on the errors in the coefficients of angular distribution of the fragments, $W(\theta)$. Specifically, it is low for the quadrupole component at high photon energies, where the sharp increase in the relative error of $Y_c(E_{max})$ due to decrease in c makes the accuracy of differentiation worse.

4. Finally, one of the main sources of errors in reduction of the cross sections is the interpolation used for the data on $Y(E_{max})$, which inevitably contained an element of arbitrariness, more important the greater the distance between the experimental points. This drawback is inherent, to some degree, in all known studies of photofission in beams of bremsstrahlung radiation. To establish the scale of the uncertainties, we analyzed, as in Ref. 9, several variants of the interpolation of $Y(E_{max})$.

The right-hsnd part of Fig. 5 shows the results of an analysis of several smooth test functions of $Y_c(E_{max})$ for ^{238}Pu, carried out in different ways within the limits of experimental errors. Their comparison graphically demonstrates the recorded uncertainties of the analysis. Instructive in this respect is an analysis of curve (1), which is the smoothed dependence, $\sigma_c(E)$, ignoring the irregularity of variants (2) and (3); the upper part of Fig. 5 shows its corresponding curve, $Y_c(E_{max})$, obtained by integration over the known gamma spectrum. It, obviously, cannot be rejected as not agreeing with experiment. In other words, the achieved accuracy of the experimental data does not guarantee authenticity of the "resonance" structure of the cross section. We give special attention to these effects in

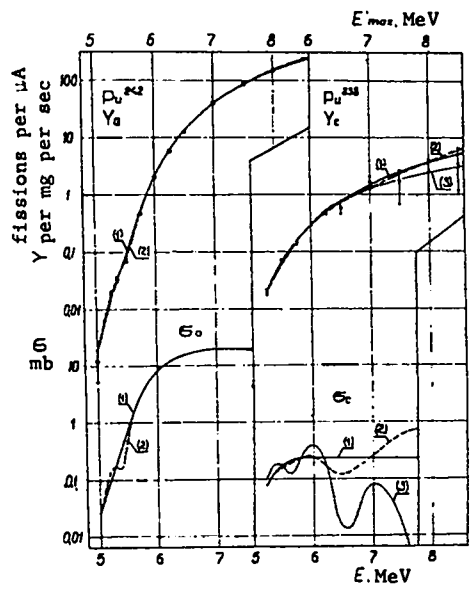

Fig. 5. Examples of variants of treatment of yields (see text).

connection with the role of quasi-stationary states in the fission process, which has been intensively discussed recently.[7,14,15]

Figure 3 shows the dependences $Y(E_{max})$ and $Y_i(E_{max})$, as well as $\sigma(E)$, which is obtained as a result of their analysis. For the quadrupole components, only the smoothed curves $\sigma_c(E)$ and $Y_c(E_{max})$, obtained by integrating them over the bremsstrahlung spectrum, are given.

Investigation of the solutions showed that:

1. The overwhelming majority of the observed dependences $Y_i(E_{max})$ and $Y(E_{max})$ within the limits of experimental error can be satisfactorily coordinated with the smoothed curves for $\sigma(E)$ in Fig. 3 (including $\sigma_a(E)$ for ^{232}Th;
2. An authentic exception is only the total, $\sigma_{\gamma f}(E)$, and the dipole, $\sigma_b(E)$, fission cross section for ^{232}Th (maximum near 5.6 MeV) and, possibly, the isotropic component, $\sigma_a(E)$, for ^{242}Pu (see Fig. 5 at left; the smoothed variant is taken in Fig. 3);
3. The low-energy portion below and near the fission threshold, < 6.5 to 7 MeV, is very reliable.

The cross sections shown in Fig. 3 are normalized over the points obtained in experiments with monochromatic gamma quanta.[16] Figure 6 gives the curves $b/a = 3/2\ \sigma_b/\sigma_a$ and $c/b = 5/4\ \sigma_c/\sigma_b$ for the nuclei studied. For ^{232}Th and ^{238}U they are compared with the results of measurements in monochromatic gamma quanta of the reactions (n,γ)[16,17] and $^{19}F\ (p,\alpha\gamma)^{16}O$.[3,18] Caution should be observed in comparing data on photofission by 6.14-MeV gamma quanta from the $^{19}F\ (p,\alpha\gamma)\ ^{16}O$ reaction with others because the width of this line is, in all, 10 eV,[19] and only one state of the compound nucleus can be excited during its photoabsorption.

DISCUSSION OF RESULTS

The principal qualitative traits of the observed angular distributions of the photofission fragments are as follows.

1. A significant decrease in the isotropic component with decreasing energy into the subbarrier region.
2. A sharp increase in the quadrupole component during the above.
3. A nonmonotonic behavior of the ratio b/a with decrease in energy.
4. A strong dependence of the energy path of the partial cross sections and their ratios (the coefficients of anisotropy) on the nucleon composition of the fissioning nucleus.

The gamma quanta, independent of the multipolarity, have a total angular momentum projection in the direction of their motion, equal in absolute value to unity; therefore, during their absorption by even-even nuclei with zero spin, states of the compound nucleus with the same preferred values $M_z = \pm 1$ are formed. If K is preserved in the fission process, then the angular distribution of the fragments, normalized by the condition

$$\int_0^{\pi} W(\theta)\, d\theta = 1,$$

has the form

$$W_K^J(\theta) = \frac{2J+1}{4(1+\delta_{K0})} \left\{ |D_{1K}^J|^2 + |D_{1-K}^J|^2 \right\}, \qquad (8)$$

where $D_K^J(\theta)$ are the spherical Wigner functions. Let us assume that the absorption of quanta occurs only with the multipolarities E1 and E2, and for the levels of compound nuclei; consequently, only two combinations, 1^- and 2^+, of spin and parity

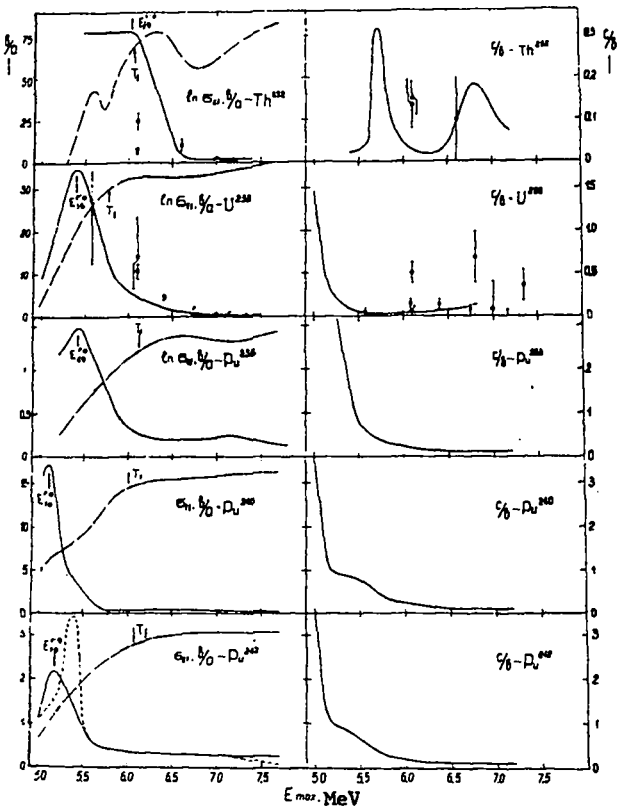

Fig. 6. Dependence of ratios b/a and c/b, obtained from curves of σ_i in Fig. 3 (solid lines) and ln $\sigma_{\gamma f}$ in arbitrary units (dash line) on energy of γ-quanta, E. Points denote results of work of Ref. 3 (o), Ref. 18 (●), and Refs. 16 and 17 (□) for b/a and c/b. Dotted line shows b/a for variant treatment leading to irregularity in σ_a for ^{242}Pu (see Fig. 5).

are possible. Thus, in the caluclations only the following elementary angular distributions of the type of Eq. (8) can be necessary.

$$W_0^1(\theta) = \frac{3}{4}\sin^2\theta \quad ,$$

$$W_1^1(\theta) = \frac{3}{4}\left(1 - \frac{1}{2}\sin^2\theta\right) \quad ,$$

$$W_0^2(\theta) = \frac{15}{16}\sin^2 2\theta \quad ,$$

$$W_2^2(\theta) = \frac{5}{8}\left(\sin^2\theta + \frac{1}{4}\sin^2 2\theta\right) \quad , \qquad (9)$$

and

$$W_1^2(\theta) = \frac{5}{4}\left(1 - \frac{1}{2}\sin^2\theta - \frac{1}{2}\sin^2 2\theta\right) \quad .$$

The differential photofission cross section has the form

$$\frac{d\sigma_{\gamma f}}{d\Omega} = \sigma_\gamma^{1^-} \sum_{K=0,1} P_K^{1^-} W_K^{1^-}(\theta) + \sigma_\gamma^{2^+} \sum_{K=0,1,2} P_K^{2^+} W_K^2(\theta) \quad . \qquad (10)$$

Here $\sigma_\gamma^{1^-}$ and $\sigma_\gamma^{2^+}$ are the cross sections of photoabsorption of dipole and quadrupole gamma quanta, respectively, and $P_K^{J\pi}$ is the probability of fission through a channel with a given K (in this it is necessary to take into account that the values of $K \neq 0$ have twice as large a statistical weight as $K = 0$). An isotropic angular distribution is obtained when all K are equally probable, which in the chosen normalization corresponds to the equality

$$\sum_{K=0}^{J} W_K^J (2 - \delta_{K0}) = \text{const} = \frac{2J+1}{2} \quad . \qquad (11)$$

If fission with different values of K is possible from a state with fixed J and π, then

$$P_K^{J\pi} = \Gamma_{fK}^{J\pi}\Big/\Big(\Gamma_c + \sum_{K'}\Gamma_{fK'}^{J\pi}\Big) \equiv \Gamma_{fK}^{J\pi}/\Gamma^{J\pi} \quad , \qquad (12)$$

where $\Gamma_{fK}^{J\pi}$ is the average fission width for a channel with fixed K and Γ_c is the total width of the compound nucleus decay processes that compete with fission. Having regrouped the terms in the angular distribution, Eq. (10), we get

$$\frac{d\sigma_{\gamma f}}{d\Omega} = \left(\frac{3}{4}\sigma_\gamma^{1^-}\frac{\Gamma_{f1}^{1^-}}{\Gamma^{1^-}} + \frac{5}{4}\sigma_\gamma^{2^+}\frac{\Gamma_{f1}^{2^+}}{\Gamma^{2^+}}\right)$$

$$+ \sin^2\theta\left(\frac{3}{4}\sigma_\gamma^{1^-}\frac{\Gamma_{f0}^{1^-}-0.5\Gamma_{f1}^{1^-}}{\Gamma^{1^-}} + \frac{5}{8}\sigma_\gamma^{2^+}\frac{\Gamma_{f2}^{2^+}-\Gamma_{f1}^{2^+}}{\Gamma^{2^+}}\right)$$

$$+ \sin^2 2\theta\,\sigma_\gamma^{2^+}\left(\frac{15}{16}\frac{\Gamma_{f0}^{2^+}}{\Gamma^{2^+}} \cdot \frac{5}{8}\frac{\Gamma_{f1}^{2^+}}{\Gamma^{2^+}} + \frac{5}{32}\frac{\Gamma_{f2}^{2^+}}{\Gamma^{2^+}}\right) . \qquad (13)$$

The main anisotropic term, proportional to $\sin^2\theta$, is ensured by a difference in the thresholds of $E_f^{J\pi K}$ to the advantage of the state 1^-, K = 0, in comparison with the state 1^-, K = 1, due to which $\Gamma_{f1}^{1^-} < \Gamma_{f0}^{1^-}$, while below the threshold with K = 1 the inequality can be strong.

The lack of reliable direct data on the absolute value and energy dependence in the considered region of total photoabsorption cross-section energy and its partial components corresponding to different multipolarities is a specific difficulty in the analysis of photofission data. Therefore, it is impossible to carry out a subsequent channel analysis, i.e., a direct extraction of the energy dependences of $\Gamma_{fK}^{J\pi}$ from experimental data, and possibilities of interpretation are limited by the need to use relative values, which are affected less by the possible inconstancy of $\sigma_\gamma^{1^-}$ and $\sigma_\gamma^{2^+}$ in the interval considered.

According to electrodynamics estimates, $\sigma_\gamma^{2^+}/\sigma_\gamma^{1^-} \approx R^2/\lambda^2$, where R is the radius of the nucleus and λ is the wavelength of a gamma quantum. For fissioning nuclei in the energy region under consideration, this ratio is about 1/20, so that a contribution of the quadrupole component ($\sim\sin^2 2\theta$) in the angular distribution comparable to the contribution of the dipole component can be obtained only for $P_0^{2^+} \gg P_0^{1^-}$. This inequality occurs when the fission barrier for the states 2^+, K = 0 is noticeably lower than that for states 1^-, K = 0, which corresponds completely to A. Bohr's fission channel model, according to which the spectrum of the channels is similar to that of the low-lying states of an even-even nucleus, and $E^{1^-} > E^{2^+}$ always. This explains the growth of both anisotropic components with decreased excitation energy. The presence of the maximum on the curve of b/a also corresponds, apparently, to a simple fact: the ratio of the penetrabilities of two barriers that differ only near the peak reverts to unity in two cases--above both barriers, when both penetrabilities are equal to unity, and in the deep subbarrier region. Consequently, for some intermediate energy, this ratio must have an extreme. Its location approximately coincides with the peak of the lower barrier. This statement is illustrated by Fig. 7. For the parabolic barriers depicted in the drawing, the ratio P_1/P_2

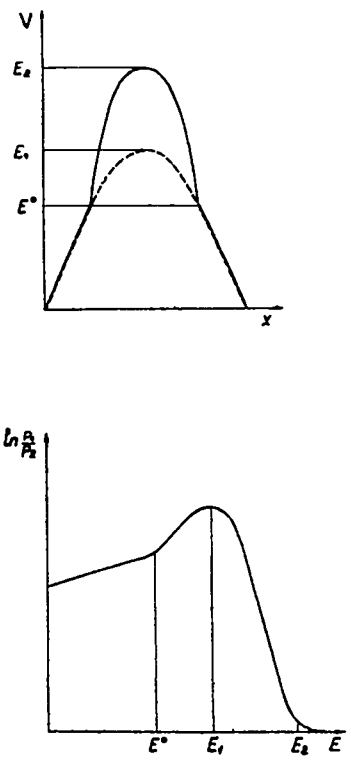

Fig. 7. Energy dependence of ratio of penetrabilities of two barriers differing only near the peak.

increases exponentially at first with decreased energy, then, after passing the maximum, for $E < E_1$ falls exponentially, but with a smaller slope. After passing the merging point of both barriers, the drop slows, but is prolonged in the limit to $P_1/P_2 = 1$.

Such is a natural qualitative explanation of the energy dependences of both anisotropic components in the cross section in the framework of traditional channel analysis. With more detailed consideration, serious difficulty arises. In the subbarrier region it must be that $\Gamma_{f0}^{J\pi} \gg \Gamma_{fK=0}^{J\pi}$. Taking into account also that $\sigma_\gamma^{1^-} \gg \sigma_\gamma^{2^+}$, from a comparison of Eqs. (2) and (13) we get that for such energies

$$b/a \sim P(1^-,0)/P(1^-,1);\ c/b \sim n\frac{P(2^+,0)}{P(1^-,0)}\ , \quad (14)$$

are approximately fulfilled where $P(J^\pi,K)$ is the penetrability of the barrier for a given combination of quantum numbers. In accordance with what has been said above, with decreased energy, b/a must reach its maximum value at about $E = E_f^{1^-,0}$, and the photofission cross section will, with increased energy, emerge onto a plateau at about the same point, more accurately, even somewhat earlier, for $E = T_f \equiv E_f^{1^-,0} - \Delta E_f$. The point T_f, the observed fission threshold, lies below the actual threshold, because the fission width becomes more competitive than the radiation width before it comes to saturation at $E = E_f^{1^-,0}$. As was shown by Usachev et al.,[20] ΔE_f is several hundred keV. This situation, predicted by fission channel theory, is depicted schematically in Fig. 8a.

In the left half of Fig. 6 the experimental results are shown in a form convenient for comparison with that predicted by theory. We see that for plutonium isotopes the point at which the anisotropy, the ratio b/a, reaches its maximum lies almost 1 MeV below the observed threshold, T_f, and must lie higher. The quantitative divergence is very sharp: the cross section at this point must approximately coincide with its value at the plateau, but actually it is approximately 100 times less. This contradiction has already been noted for ^{232}Th and ^{238}U, and in discussing yield measurements during fission of these elements in the spectrum we noted it as difficult to explain by the traditional representations.[3,5,6] Although data on the cross sections of plutonium isotopes were lacking, the fact that T_f for ^{232}Th and ^{238}U is approximately equal to $E_f^{1^-,0}$, and not less, could be explained by the assumption of spproximate preservation of the quantum number K in the states of the compound nucleus[5] or by Wilets' concept of the suppression of fission through channels corresponding to K = 0.[3] After obtaining the results for plutonium isotopes given here, we found that such explanations are not well-grounded, because, definitely, $T_f > E_f^{1^-,0}$ and the difference is significant. Just this, as we will now show, is to be expected in the double-humped barrier model for $E_{fA} > E_{fB}$ (see Fig. 8b).

The solution of the one-dimensional quasiclassical problem of the penetrability of a double-humped barrier shows[21] that the average penetrability is the same as if only barrier A existed; i.e., the location of the observed threshold in the cross section is determined by the higher barrier, A. The mechanism of the origination of anisotropy in this case, according to Strutinskii and Bjornholm,[7] is as follows. Having overcome the first barrier, the nucleus passes into the second time well far enough to "forget" the K value with which it went through the first barrier. Therefore, for $E_{fB}^{1^-,0} < E < E_{fA}^{1^-,0} < E_{fA}^{1^-,1}$ the nuclei fall into the second well through the channel $1^-,0$ in barrier A, because it is energetically favorable, and then split, and the angular distribution is determined by the location of the excitation energy relative to the channels of barrier B. In this case, T_f approximately coincides with $E_{fA}^{1^-,0}$ for barrier A (or is somewhat below this threshold), and the maxima of the ratios b/a and c/b are located approximately at energies equal to $E_{fB}^{1^-,0}$ and $E_{fB}^{2^+,0}$ (see Fig. 8b). The experimental picture corresponds completely satisfactorily to such a description, and from its analysis the threshold values given in Table III are obtained. The value $\Delta_{AB} = T_f - E_{fB}^{1^-,0}$ increases from thorium to plutonium, according to the predictions of Ref. 7. Because in most cases c/b increases monotonically with decreased energy and

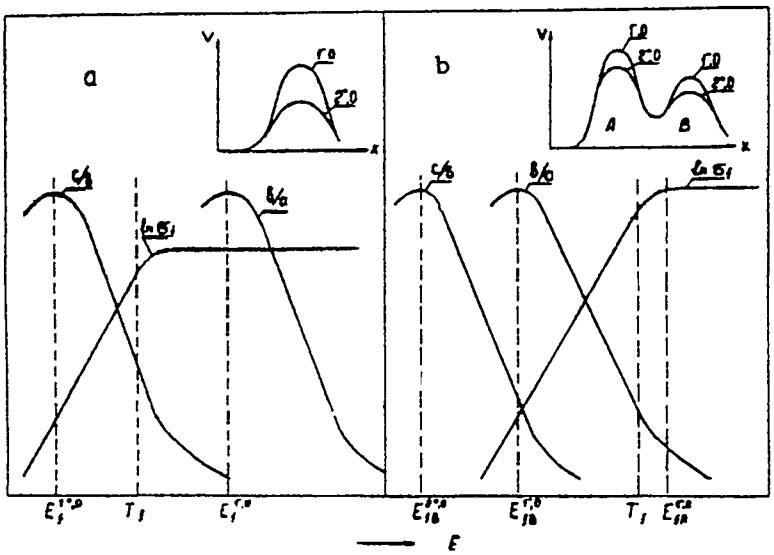

Fig. 8. Dependences of anisotropy and photofission cross section for single- (a) and double-humped (b) barriers.

TABLE III

PARAMETERS OF FISSION BARRIER AND RATIO OF CROSS SECTIONS OF DIPOLE AND QUADRUPOLE PHOTOABSORPTION*

	$E_{fB}^{2^+,0}$	$E_{fB}^{1^-,0}$	$T_f\ (\leq E_{fA}^{1^-,0})$	Δ_{AB}	r
	MeV	MeV	MeV	MeV	
Th^{232}	5.7	6.0	6.0	0	I/60
U^{238}	< 5.0	5.4	5.8	0.4	I/30
Pu^{238}	< 5.2	5.4	6.I	0.7	I/I0
Pu^{240}	< 5.0	5.I	6.0	0.9	I/I5
Pu^{242}	< 5.0	5.2	6.I	0.9	I/I0

*The characteristics given should be considered estimates having an accuracy of ~0.2 MeV.

in the last points of "b," within the limits of error, as a rule, is equal to zero, the upper limiting values for $E_{fB}^{2^+,0}$ determined by the location of the maximum of this ratio are given in Table III. Note that the presence of maxima on the curves b/a(E) occurs with monotonic decrease in σ_b with decreased energy, and, therefore, first of all, is not related to the resonance-type irregularities that can be seen in the energy dependences of the fission widths.[7,14,15]

The effects discussed above, which we relate to the possibility of existence of a second minimum in the potential surface of the fissioning nucleus, can exist only with an appreciable difference in the thresholds of A and B and a significant depth of the well between them. They, in short, reduce to superbarrier effects in the angular distributions appearing in the region that is subbarrier with respect to the cross section. This phenomenon appears clearly also during the fission of the even-even nuclei ^{234}U, ^{236}U, and ^{240}Pu in (d,pf) and (t,pf) reactions.[22] The maximum of the angular anisotropy, related to the fission through the state $K^\pi = 0^+$, is located below the neutron binding energy and corresponds to the fission probability $P \approx \Gamma_f/\Gamma_c \ll 1$, i.e., to a very small penetrability $p \ll P$, because Γ_c is equal to the radiation width. Analogous features were also noted in the fission of nuclei by neutrons.[7,23]

The nuclei studied differ strongly in the magnitude of displacement, Δ_{AB}; angular anisotropy, b/a; and the relation of the angular components near the observed threshold. The absence of a significant difference between T_f and $E_f^{1^-,0}$ and the relation $\sigma_a/\sigma_b \ll 1$ for ^{232}Th correspond with the generally accepted concepts of channel effects. This case, evidently, corresponds to a barrier for which $E_{fB} \geq E_{fA}$. The presence of a resonance in σ_b at $E \approx 5.6$ MeV[7] confirms the existence of a well between the maxima. For plutonium isotopes Δ_{AB} is large, and, as a result, even near the observed threshold, $\sigma_a/\sigma_b \gg 1$. To describe the energy dependences and the average fission widths we must use a statistical approach that agrees with the results of investigation of the angular distributions of the fragments during fission by neutrons.[23] The behavior of the indicated values for ^{238}U is intermediate. The competition from the side of emission of photoneutrons for ^{232}Th is great; for plutonium isotopes it is hardly noticeable, which is also naturally related with the difference in Δ_{AB} and, consequently, the number of states participating in fission near T_f.

An estimate of the ratio of photoabsorption cross sections of different multipolarity $\tau = \sigma_\gamma^{2^+}/\sigma_\gamma^{+}$ is of definite interest. In an earlier paper,[3] this ratio was estimated in the detailed traditional representations of a channel structure for the fission barrier. The values vary from 0.015 for ^{232}Th to 0.15 for ^{240}Pu. Table III gives the values of $\tau \approx \sigma_c/\sigma_b$.

Let us briefly enumerate our physical conclusions.

1. The energy dependence of both anisotropic components in the angular distributions agrees with the predictions of the collective model regarding the dependence of the height of the fission barrier on the quantum characteristics of the fissioning nucleus.
2. The large anisotropy values in the deep subbarrier region serve as a strong argument for the advantage of the hypothesis of the presence of a second maximum in the potential curve describing the fission barrier.
3. The ratio of the cross sections of quadrupole and dipole photoabsorption for heavy even-even nuclei near 5- to 6-MeV energies is close to 1/20, in qualitative agreement with electrodynamic estimates.

ACKNOWLEDGMENTS

We are deeply grateful to P. L. Kapitsa for support of our studies, to V. M. Strutinskii for valuable discussions, and to M. K. Golubeva and N. E. Fedorova for participation in the work.

REFERENCES

1. E. J. Winhold, P. T. Demos, and I. Halpern, Phys. Rev. 87, 1139 (1952).
2. A. Bohr, Proc. Intern. Conf. Peaceful Uses At. Energy, Geneva, 1955, Vol. 2, p. 151.
3. N. S. Rabotnov, G. N. Smirenkin, A. S. Soldatov, L. N. Usachev, S. P. Kapitsa, and Iu. M. Tsipeniuk, Physics and Chemistry of Fission, Vol. 1, IAEA, Vienna, 1965, p. 135.
4. I. E. Bocharova, V. G. Zolotuzhin, S. P. Kapitsa, G. N. Smirenkin, A. S. Soldatov, and Iu. M. Tsipeniuk, Zh. Eksperim. i Teor. Fiz. 49, 476 (1965).

5. N. S. Rabotnov, G. N. Smirenkin, A. S. Soldatov, L. N. Usachev, S. P. Kapitsa, and Iu. M. Tsipeniuk, Phys. Lett. 26B, 218 (1968).

6. S. P. Kapitsa, N. S. Rabotnov, G. N. Smirenkin, A. S. Soldatov, L. N. Usachev, and Iu. M. Tsipeniuk, Zh. Eksperim. i Teor. Fiz. Pis'ma 9, 128 (1969).

7. V. M. Strutinskii and S. Bjornholm, Intern. Symp. Nuclear Structure, Dubna, 1968.

8. A. S. Soldatov, I. E. Bocharova, and G. N. Smirenkin, Pribory i Tekhn. Eksperim. 5, 226 (1968).

9. L. Katz, A. P. Baerg, and F. Brown, Proc. UN Intern. Conf. Peaceful Uses At. Energy, 2nd, Geneva, 1958, Vol. 15, p. 188.

10. J. D. Lawson, Nucleonics 10, No. 11, 61 (1952).

11. N. Starfelt and H. W. Koch, Phys. Rev. 102, 1598 (1956).

12. M. H. MacGregor, Nucleonics 15, No. 11, 176 (1957).

13. V. F. Turchin, Zh. Vychislitel'noi Matematiki i Matematicheskoi Fiziki 8, 230 (1968); V. Z. Nozik and V. F. Turchin, Preprint FEI-138.

14. J. E. Lynn, Nuclear Data for Reactors, Proc. Conf. on Nuclear Data, Microscopic Cross-Sections and Other Data Basic for Reactors, Paris, 1966. IAEA, Vienna, 1967, Vol. 2, p. 89.

15. P. E. Vorotnikov, S. M. Dubrovina, G. A. Otroshchenko, and V. A. Shigin, Iadern. Fiz. 7, 1228 (1968); Iadern. Fiz. 5, 295 (1967).

16. A. Manfredini, L. Fiore, C. Ramorino, H. G. de Carvalho, and W. Wölfli, Nucl. Phys. A123, 664 (1969).

17. H. G. de Carvalho, A. Manfredini, M. Muchnik, M. Severi, R. Bösch, and W. Wölfli, Nuovo Cimento 29, 464 (1963).

18. B. Forkman and S. A. E. Johansson, Nucl. Phys. 20, 136 (1960).

19. J. R. Huizenga, K. M. Clarke, J. E. Gindler, and R. Vandenbosch, Nucl. Phys. 34, 439 (1962).

20. L. N. Usachev, V. A. Pavlinchuk, and N. S. Rabotnov, At. Energ. USSR 17, 479 (1964).

21. E. V. Gai, A. B. Ignatiuk, N. S. Rabotnov, and G. N. Smirenkin, Preprint FEI-158.

22. H. C. Britt, F. A. Rickey, Jr., and W. S. Hall, Preprint LA-DC-9562 (1968); published in Phys. Rev. 175, 1525 (1968).

23. Kh. D. Androsenko and G. N. Smirenkin, Zh. Eksperim. i Teor. Fiz. Pis'ma 8, 181 (1968). D. L. Shpak and G. N. Smirenkin, Zh. Eksperim. i Teor. Fiz. Pis'ma 9, 196 (1969).